I. *J. Phys. Chem.* **1990**, *94*, 5652.
10. Sanchez, C.; In M. *J. Non-Cryst. Solids* **1992**, *147&148*, 1.
11. Negishi, N.; Fujii, T.; Anpo, M. *Langmuir* **1993**, *9*, 3320.
12. See, for example, *Photochemistry in Organized and Constrained Media*; Ramamurthy V. Ed.; (1991) VCH Publishers, 1991.
13. Forster, T. *Angew. Chem.* **1969**, *8*, 333.
14. Hara, K.; Yano, H. *J. Am. Chem. Soc.* **1988**, *110*, 1911.
15. Snare, M. J.; Thistlethwaite, P. J.; Ghiggino, K. P. *J. Phys. Chem.* **1983**, *105*, 3328.
16. Reynders, P.; Kuhnle, W.; Zachariasse, K. A. *J. Phys. Chem.* **1990**, *94*, 4073.
17. Tsuchida, A.; Ikawa, T.; Tomie, T.; Yamamoto, M. *J. Phys. Chem.* **1995**, *99*, 8196.

Channel Electrode Voltammetric and *In Situ* Electrochemical ESR Studies of Comproportionation of Methyl Viologen in Acetonitrile

Chi-Woo Lee*†, John C. Eklund‡, Robert A. W. Dryfe‡, and Richard G. Compton‡

†*Department of Chemistry, College of Natural Sciences, Korea University, Jochiwon, Choongnam 339-700*
‡*Physical and Theoretical Chemistry Laboratory, Oxford University, South Parks Road, Oxford. OX1, United Kingdom*

Received October 14, 1995

Two redox processes of methyl viologen (+2/+, +/0) in acetonitrile were investigated by using channel electrode voltammetric and in situ electrochemical ESR methods. Two separated unequal plateau currents of the first (+2/+) and second (+/0) redox processes of the viologen were observed in the channel electrode voltammograms and showed a cube-root depedndence on the electrolyte flow rate, respectively. The simple Levich analysis resulted in two different diffusion coefficients of $D_{+2}=2.2\times10^{-5}$ cm²/s and $D_{+}=3.0\times10^{-5}$ cm²/s from the limiting currents. *In situ* electrochemical ESR studies were performed for the monocation radicals generated at the potentials of the two plateau currents in the electrolyte flow range $1.3\times10^{-1}\geq v_f \geq 2.7\times10^{-3}$ cm³/s. Backward implicit finite difference method was employed to simulate the electrochemical kinetic problem of two sequential electron transfers ($MV^{+2}+e \rightleftarrows MV^{+}$, $MV^{+}+e \rightleftarrows MV^{o}$) coupled with reversible comproportionation ($MV^{2+}+MV^{o} \underset{k_b}{\overset{k_f}{\rightleftarrows}} 2MV^{+}$). k_f was found to be greater than 10^6 M^{-1} s^{-1}.

Introduction

As part of continuing studies of understanding the thermodynamic aspects of and electrochemical kinetic effects by asymmetric surfactant viologens in organized molecular assemblies,[1,2] we have investigated the following two reductive electrochemical processes of viologens (V^{+2}) coupled with comproportionation in acetonitrile solutions by using channel electrodes.

$$V^{+2}+e^{-} \rightleftarrows V^{+} \qquad E^{o'}_{+2/+} \qquad (1)$$

$$V^{+}+e^{-} \rightleftarrows V^{o} \qquad E^{o'}_{+/o} \qquad (2)$$

$$V^{o}+V^{+2} \rightleftarrows 2V^{+} \qquad K \qquad (3)$$

Since the formal potentials of reactions (1) and (2), $E^{o'}_{+2/+}$ and $E^{o'}_{+/o}$, are separated by several tenths of a volt with $E^{o'}_{+2/+}$ less negative than $E^{o'}_{+/o}$, the thermodynamically spontaneous comproportionation between V^{o} and V^{+2} produces the singly-reduced radical cation, which shows a strong ESR signal, at the potential corresponding to the overall $2e^{-}$ reduction of V^{+2}. Thus electrochemical method combined with ESR spectroscopy will be a method of choice to approach to solve the kinetic problem.

The channel electrode,[3] which utilizes the well-defined flow pattern inside the channel and the efficient numerical method of backward implicit finite difference (BIFD) for the geometry of channel flow cells, has been proved to be a useful hydrodynamic electrode for the mechanistic investigation of the electrode reactions which involve homogeneous chemical reactions. It consists of an electrode embedded in the wall of a rectangular duct through which electrolyte solution is flowed, as shown in Figure 1.

In situ electrochemical ESR method using the channel electrode has been successfully applied to tackel an irreversible comproportionation system by Compton.[4] The present work is to consider reversible comproportionation reaction by using channel electrode voltammetric and *in situ* electrochemical ESR methods experimentally and theoretically.

Comproportionation kinetics of methyl viologen has been studied by several different groups previously.[5~7] Our results agree with the reaction scheme (1)-(3) and large comproportionation rate constant (k_f) reported by others, and nonidentical plateau currents of the first and second redox processes and unequal diffusion coefficients of the viologen dication

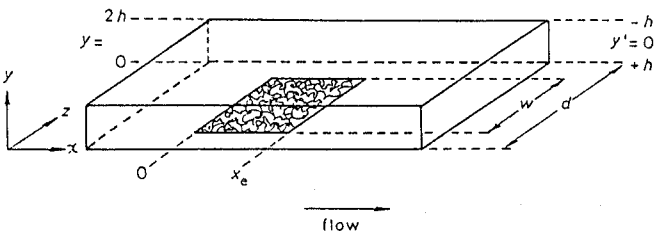

Figure 1. The coordinate system of the channel electrode used in Theory.

and monocaion obtained in the present work are a new addition to the comproportionation kinetics of the system.

Experimental

All reagents were of the best commercial quality available. Methyl viologen hexefluorophosphate ($MV(PF_6)_2$) was prepared by metathesis of the corresponding chloride salt (Aldrich) with ammonium hexafluorophosphate (Sigma). The resulting precipitate was recrystallized from H_2O. Tetrabutylammonium perchlorate (TBAP) was recrystallized from ethylacetate and dried under vacuum.

All of the electrochemical experiments were performed under an argon atmosphere. An Oxford electrode potentiostat and Lloyd instrument recorder were employed for voltammetric measurements. The ESR spectrometer used in this work was a Bruker ER 200D equipped with a 9-inch (23 cm) magnet, a rectangular TE_{102} cavity and a field-frequency lock. All data were recorded with the electrode located centrally in the cavity in the absence and presence of magnetic field applied.

In situ electrochemical ESR measurements were made using a demountable channel flow electrode unit built in synthetic fused quartz (Silica and Metals Ltd., Surrey, U.K.) to a design previously described.[12,13] Diamond lapping compounds (Engis, Maidstone, U.K.) were used to polish the gold foil electrode of 0.360×0.319 cm, which was cemented onto the central silica cover plate by using all purpose Bostik glue (Leicester, U.K.). Precise values of the cell dimensions were measured using a travelling microscope. The channel unit was supported within a standard rectangular TE_{102} ESR cavity by means of PTFE spacers inside a silica tube, which ran right through the ESR cavity and which was held by nylon collets.

The cell position within the cavity could be finely adjusted by movement of the supporting tube and the electrode was positioned centrally in the cavity so that it was at the position of the highest ESR sensitivity. The assembled channel unit was attached to a gravity-fed flow system with a platinum gauze counter electrode located outside the cavity downstream of the working electrode and 20 cm remote from it to preclude counter electrode products diffusing to the working electrode. A purpose-built potentiostat of modular construction to derive the current through the resistive channel was used throughout.[14] It has been previously established that no counter electrode products entered the cavity within 60 min of commencing electrolysis in this design.[15] A silver wire quasireference (AgQRF) electrode was located in the flow system upstream of the cavity. Reported potentials were taken only when they were reproducible from repeated experiments at different flow rate and are quoted versus AgQRF.

Numerical simulations utilized the BIFD method which was facilitated with the Thomas algorithm.[3,8~10] Advantages of BIFD over the standard explicit finite difference method and the Crank-Nicholson method has been clearly illustrated for solving problems of the channel electrode by Anderson.[9] A grid size of 10,000×2,000 (K×J) over the zone of the electrode and a correspondingly spaced grid downstream was employed so as to give accurate and converged results. Transport of all species was assumed to be described by the convective-diffusion equation.

Results and Discussion

Theory. In this section we describe the theoretical models for the channel electrode voltammetry and *in situ* electrochemical ESR on the reversible comproportionation kinetics. For simplicity, we focus our attention on the reduction only.

$$A + e^- \rightleftarrows B \qquad E^{o'}_{A/B} \qquad (4)$$

$$B + e^- \rightleftarrows C \qquad E^{o'}_{B/C} \qquad (5)$$

$$C + A \underset{k_b}{\overset{k_f}{\rightleftarrows}} 2B \qquad K_{comp} \qquad (6)$$

We assume that $E^{o'}_{A/B}$ is more positive than $E^{o'}_{B/C}$ and that $K_{comp}=\exp[-F/RT(E^{o'}_{B/C}-E^{o'}_{A/B})]$ is sufficiently large. The time-dependent mass transport to the electrode surface in the presence of an adequate quantity of supporting electrolyte is described by the convective-diffusion equation as follows.

$$\frac{\partial[A]}{\partial t}=D_A\frac{\partial^2[A]}{\partial y^2}-v_x\frac{\partial[A]}{\partial x}-k_f[A][C]+k_b[B]^2 \qquad (7)$$

$$\frac{\partial[B]}{\partial t}=D_B\frac{\partial^2[B]}{\partial y^2}-v_x\frac{\partial[B]}{\partial x}+2k_f[A][B]-2k_b[B]^2 \qquad (8)$$

$$\frac{\partial[C]}{\partial t}=D_C\frac{\partial^2[C]}{\partial y^2}-v_x\frac{\partial[C]}{\partial x}-k_f[A][C]+k_b[B]^2 \qquad (9)$$

where x and y are defined in Figure 1, and v_x represents the solution velocity profile in the x-direction. Other symbols have their usual meanings. The solution velocity profile in the x-direction is, when a sufficiently long lead-in section is present for the flow to become fully developed, given by

$$V_x=V_o\left(1-\left(\frac{y'}{h}\right)^2\right)$$

where V_o is the velocity at the center of the channel, $y'=h-y$ and h is the half-height of the channel. With the introduction of the dimensionless concentrations of $a=[A]/[A]_o$, $b=[B]/[A]_o$ and $c=[C]/[A]_o$, the steady-state convective-diffusion equations become

$$D_A\frac{\partial^2 a}{\partial y^2}=V_x\frac{\partial a}{\partial x}+k_f\ a\ c\ [A]_o-k_b\ b^2[A]_o \qquad (10)$$

$$D_B\frac{\partial^2 b}{\partial y^2}=V_x\frac{\partial b}{\partial x}-2k_f\ a\ c\ [A]_o+k_b\ b^2[A]_o \qquad (11)$$

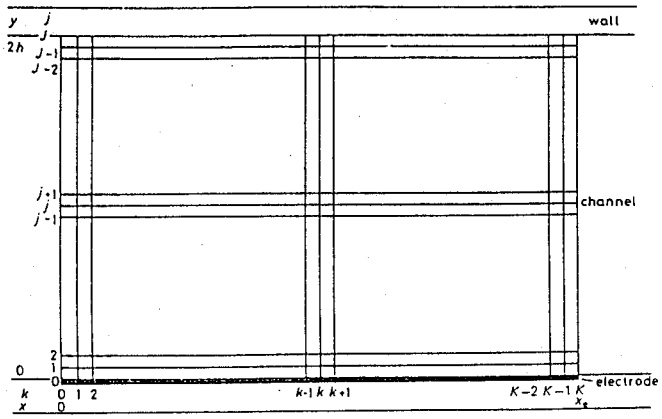

Figure 2. The finite difference grid for backward implicit finite difference method.

$$D_C\frac{\partial^2 c}{\partial y^2}=V_x\frac{\partial c}{\partial x}+k_f\ a\ c\ [\mathrm{A}]_o-k_b\ b^2[\mathrm{A}]_o \tag{12}$$

The boundary conditions to calculate concentrations are

$x<0$ all y; $a=a_{bulk}$ $b=c=0$

$0<x<x_e$ $y=0$;

$$D_A\frac{\partial a}{\partial y}+D_B\frac{\partial b}{\partial y}+D_C\frac{\partial c}{\partial y}=0$$

$$a/b=\exp(\theta_{A/B}),\ b/c=\exp(\theta_{B/C})$$

$$\theta_{s/s'}=\frac{F}{RT}(E-E^o_{s/s'})$$

all x $y=2h$;

$$\frac{\partial a}{\partial y}=\frac{\partial b}{\partial y}=\frac{\partial c}{\partial y}=0$$

To solve the equations (10)-(12), we utilizes BIFD method.[3,8~10] This approach necessitates the adoption of the two-dimensional finite-difference grid shown in Figure 2 which covers the xy plane. There are increments Δx and Δy in the x and y directions respectively so that

$$y=j\Delta y\ \ j=0,\ 1,\ 2,\cdots J \text{ where } \Delta y=\frac{2h}{J}$$

$$x=k\Delta x\ \ k=0,\ 1,\ 2,\cdots K \text{ where } \Delta x=\frac{x_e}{K}$$

We use the symbol $a_{j,k}$, $b_{j,k}$ and $c_{j,k}$ to denote the concentrations of A, B and C at the coordinate (j, k) so that, in finite-difference form, the steady state transport equations (10)-(12) become

$$a_{j,k}\left(1-\frac{(\Delta y)^2}{D_A}\lambda_j^a\ k_f\ c_{j,k}[\mathrm{A}]_o\right)+\frac{(\Delta y)^2}{D_A}\lambda_j^a\ k_b\ b_{j,k}\ b_{j,k}[\mathrm{A}]_o$$
$$=-\lambda_j^a\ a_{j-1,k+1}+(2\lambda_j^a+1)\ a_{j,k+1}-\lambda_j^a\ a_{j+1,k+1} \tag{13}$$

$$b_{j,k}\left(1-\frac{2(\Delta y)^2}{D_B}\lambda_j^b\ k_b\ b_{j,k}[\mathrm{A}]_o\right)+\frac{2(\Delta y)^2}{D_B}\lambda_j^b\ k_f\ a_{j,k}\ c_{j,k}[\mathrm{A}]_o$$
$$=-\lambda_j^b\ b_{j-1,k+1}+(2\lambda_j^b+1)\ b_{j,k+1}-\lambda_j^b\ b_{j+1,k+1} \tag{14}$$

$$c_{j,k}\left(1-\frac{(\Delta y)^2}{D_C}\lambda_j^c\ k_f\ a_{j,k}[\mathrm{A}]_o\right)+\frac{(\Delta y)^2}{D_C}\lambda_j^c\ k_b\ b_{j,k}\ b_{j,k}[\mathrm{A}]_o$$
$$=-\lambda_j^c\ c_{j-1,k+1}+(2\lambda_j^c+1)\ c_{j,k+1}-\lambda_j^c\ c_{j+1,k+1} \tag{15}$$

where $\lambda_j^s=\dfrac{(2h)^3 d(\Delta x)D_s}{6v_f(2h-j(\Delta y))j(\Delta y)^3}$ for $s=a,\ b$ and c.

These three $(J-1)$ simultaneous equations can be expressed as $(J-1)\times(J-1)$ matrices, *i.e.*,

$$\begin{bmatrix} d_1^s \\ d_2^s \\ d_3^s \\ \cdot \\ \cdot \\ \cdot \\ d_{J-1}^s \end{bmatrix} = \begin{bmatrix} b_1^s & -\lambda_1^s & & & 0 \\ -\lambda_2^s & 2\lambda_2^s+1 & -\lambda_2^s & & \\ & \cdot & \cdot & \cdot & \\ & & \cdot & \cdot & \cdot \\ & & & \cdot & \cdot \\ & & & -\lambda_{J-2}^s & 2\lambda_{J-2}^s \\ 0 & & & -\lambda_{J-2}^s & \lambda_{J-1}^s+1 \end{bmatrix} \begin{bmatrix} S_{1,k+1} \\ S_{2,k+1} \\ \\ \\ \\ \\ S_{J-1,k+1} \end{bmatrix}$$

The matrix elements d_1, d_j and b_1 are

$$d_1^a=a_{1,k}\left(1-\frac{(\Delta y)^2}{D_A}\lambda_1^a k_f c_{1,k}[\mathrm{A}]_o\right)+\frac{(\Delta y)^2}{D_A}\lambda_1^a k_b\ b_{1,k}\ b_{1,k}[\mathrm{A}]_o$$
$$+\frac{\lambda_1^a\exp(\theta_{A/B})[b_{1,k+1}+\frac{D_C}{D_B}c_{1,k+1}]}{\mathrm{FUNC}}$$

$$d_j^a=a_{j,k}\left(1-\frac{(\Delta y)^2}{D_A}\lambda_j^a k_f c_{j,k}[\mathrm{A}]_o\right)+\frac{(\Delta y)^2}{D_A}\lambda_j^a k_b\ b_{j,k}\ b_{j,k}[\mathrm{A}]_o$$

$$b_1^a=1+\lambda_1^a\left(2-\frac{\exp(\theta_{A/B})\left(\frac{D_A}{D_B}\right)}{\mathrm{FUNC}}\right)$$

$$d_1^b=b_{1,k}\left(1-2\frac{(\Delta y)^2}{D_B}\lambda_1^b\ k_b\ b_{1,k}[\mathrm{A}]_o\right)+\frac{2(\Delta y)^2}{D_B}\lambda_1^b\ k_f\ a_{1,k}\ c_{1,k}[\mathrm{A}]_o$$
$$+\lambda_1^b\left(\frac{D_A}{D_B}a_{1,k+1}+\frac{D_C}{D_B}C_{1,k+1}\right)/\mathrm{FUNC}$$

$$d_j^b=b_{j,k}\left(1-2\frac{(\Delta y)^2}{D_B}\lambda_j^b\ k_b\ b_{j,k}[\mathrm{A}]_o\right)+\frac{2(\Delta y)^2}{D_B}\lambda_j^b\ k_f\ a_{j,k}\ c_{j,k}[\mathrm{A}]_o$$

$$b_1^b=1+\lambda_1^b\left(2-\frac{1}{\mathrm{FUNC}}\right)$$

$$d_1^c=c_{1,k}\left(1-\frac{(\Delta y)^2}{D_C}\lambda_1^c k_f\ a_{1,k}[\mathrm{A}]_o\right)+\frac{(\Delta y)^2}{D_C}\lambda_1^c\ k_b\ b_{1,k}\ b_{1,k}[\mathrm{A}]_o$$
$$+\frac{\lambda_1^c\ \exp(-\theta_{B/C})\left(\frac{D_A}{D_B}a_{1,k+1}+b_{1,k+1}\right)}{\mathrm{FUNC}}$$

$$d_j^c=c_{j,k}\left(1-\frac{(\Delta y)^2}{D_C}\lambda_j^c k_f\ a_{j,k}[\mathrm{A}]_o\right)+\frac{(\Delta y)^2}{D_C}\lambda_1^c k_b\ b_{j,k}\ b_{j,k}[\mathrm{A}]_o$$

$$b_1^c=1+\lambda_1^c\left(2-\frac{\exp(-\theta_{B/C})\left(\frac{D_C}{D_B}\right)}{\mathrm{FUNC}}\right)$$

where $\mathrm{FUNC}=\dfrac{D_A}{D_B}\exp(\theta_{A/B})+1+\dfrac{D_C}{D_B}\exp(-\theta_{B/C})$

The matrix equations can be solved efficiently by using the Thomas algorithm. Because of the $y=0$ boundary conditions, the three simultaneous equations are interdependent, *i.e.*, we can only find $a_{j,k+1}$ with a knowledge of $b_{1,k}$ and $c_{1,k}$ or $b_{j,k+1}$ with $c_{1,k}$ and $a_{1,k}$ or $c_{j,k+1}$ with $a_{1,k}$ and $b_{1,k}$. An iterative method was employed, whereby, $a_{1,k+1}$, and $b_{1,k+1}$ was approximated by $a_{1,k}$ and $b_{1,k}$, respectively, in order to calculate $c_{j,k+1}$. The obtained $c_{j,k+1}$ with $b_{1,k+1}$ approximated by $b_{1,k}$ was used to get a better value for $a_{j,k+1}$. Then the obtained $c_{j,k+1}$ and $a_{j,k+1}$ was used to calculate a better value for $b_{j,k+1}$. The

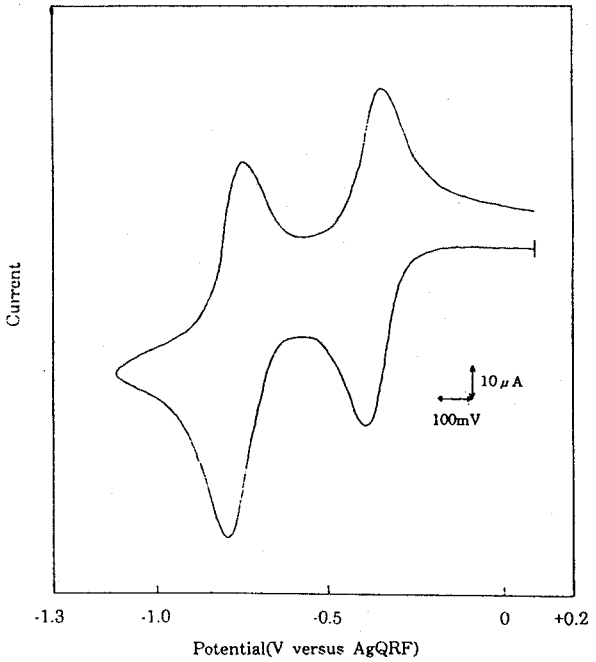

Figure 3. Cyclic voltammogram of 1.0 mM $MV(PF_6)_2$ at a gold channel electrode in CH_3CN+0.1 M TBAP at v_f=0. Scan rate, 100 mV/s. The initial potential was +0.1 V versus AgQRF. The cathodic current was plotted downward.

procedure was continued until $a_{1,k+1}$, $b_{1,k+1}$ and $c_{1,k+1}$ values were unchanged on further iteration.

The expression for the current, I, at the electrode is given by

$$I=-wF\int_0^{x_e}\left[2D_A\left(\frac{\partial a}{\partial y}\right)_{y=0}+D_B\left(\frac{\partial b}{\partial y}\right)_{y=0}\right]\,dx$$

$$\text{or}\quad =-wF\int_0^{x_e}\left[2D_C\left(\frac{\partial c}{\partial y}\right)_{y=0}+D_B\left(\frac{\partial b}{\partial y}\right)_{y=0}\right]\,dx$$

$$\text{or}\quad =-wF\int_0^{x_e}\left[2D_C\left(\frac{\partial a}{\partial y}\right)_{y=0}-D_A\left(\frac{\partial a}{\partial y}\right)_{y=0}\right]\,dx$$

assuming that the redox couples A/B and B/C are electrochemically reversible and that the electrode current is solely governed by diffusive fluxes. F is Faraday constant and w is the width of electrode.

The ESR signal can be obtained by taking the integral of the concentration of ESR active B over the whole volume of the ESR cavity weighted by a $\cos^2$ sensitivity profile along the length of the cavity.[4,16] The following equation shows the individual contributions to the ESR signal (S) from the cavity spaces adjacent to and downstream from the electrode:

$$S=P\int_0^{2h}\int_{(-Xe/2)+x_{offset}}^{(Xe/2)+x_{offset}}\left(b\cos^2\left(\frac{\pi x}{2x_L}\right)+\int_{(-Xe/2)+x_{offset}}^{x_L} b\cos^2\left(\frac{\pi x}{2x_L}\right)\right)dxdy$$

where P is a constant, $2x_L$ is the length of the ESR cavity and x_{offset} is the offset-distance from the center.

Experiments

Figure 3 shows a cyclic voltammogram obtained at the channel electrode with the acetonitrile solution containing 1.0 mM $MV(PF_6)_2$ and 0.1 M TBAP at v_f=0. The voltammogram is characterized by the two cathodic and corresponding anodic peaks resulting from the two stepwise reductions of viologen dication and reoxidations (1) and (2), respectively.[7] The unequal cathodic peak currents and corresponding anodic peaks may reflect that the homogeneous reversible charge transfer reaction (3) is involved in the electrochemical reaction. The same effect of the comproportionation of viologens is seen in the channel electrode voltammograms shown in Figure 4. The second plateau current was always greater than the first one at the given flow rate and the ratio of the second to first plateau current was 1.24 with little dependence on electrolyte flow rate, indicating that the diffusion coefficients of methyl viologen dication, monocation and neutral forms (D_{+2}, D_+, D_o) are not identical in acetonitrile media. This is in apparent contradiction with the observation under diffusion-only conditions at a platinum microdisk electrode by White[7] that the transport-limited current for the $2e^-$ reduction of methyl viologen dication is twice that for the $1e^-$ reduction but is in agreement with the recent report by Evans[17] that the current for a two-electron reaction is not necessarily twice that of a one-electron reaction when the comproportionation reaction involved is very rapid. The comproportionation reaction (3) is reported to be essentially diffusion-controlled.[5~7] The molecular mass of viologen dication, monocation and neutral forms is the same and the charge is two, one and zero, respectively so that it is expected to be $D_{+2}<D_+<D_0$. White has established that the only heterogeneous reaction involved in the steady-state reduction of methyl viologen dication is simply the one e^- reduction of the monocation.[7] Also, because neutral viologen always diffuses away from the electrode, the value of D_o will not have a direct effect on the current which, in fact, arises from the transport of viologen dication and monocation toward the electrode surface. The transport-limited currents for the first and second redox process in the channel electrode voltammograms were found to be proportional to a cube-root of solution flow rate, respectively and the values for the diffusion coefficients of $D_{+2}=2.2(\pm 0.2)\times10^{-5}$ cm^2/s and $D_+=3.0(\pm 0.3)\times10^{-5}$ cm^2/s were derived from a simple Levich analysis. We attempted without success to determine the diffusion coefficients of D_+ and D_o separately by rotating disk

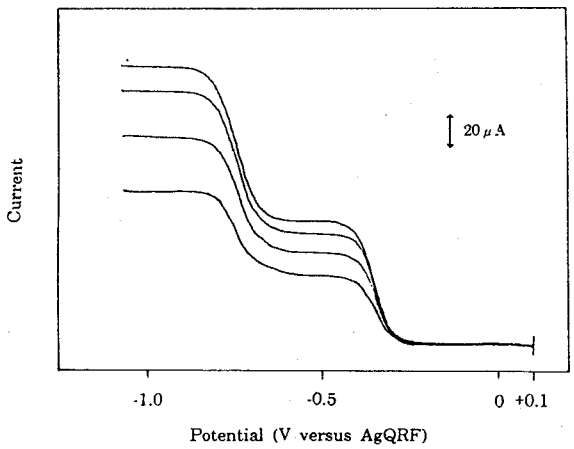

Figure 4. Representative channel electrode voltammograms at $v_f=1.83\times10^{-2}$, 2.69×10^{-2}, 8.44×10^{-2} and 1.22×10^{-1} mL/s. Other conditions are the same as Figure 3.

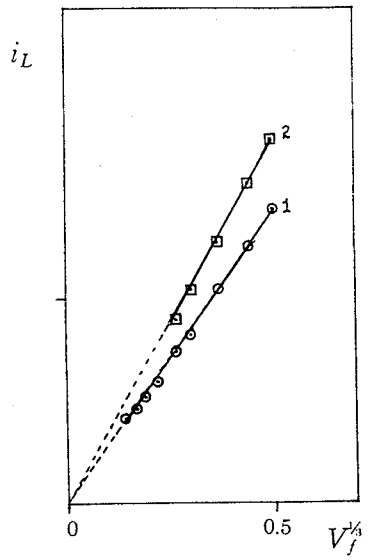

Figure 5. Levich plots of the first (1) and second (2) plateau currents of the channel electrode voltammograms.

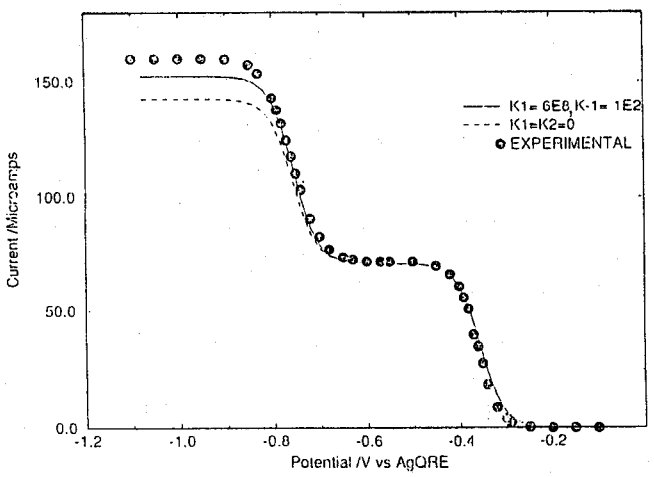

Figure 6. Experimental (·) and simulated channel electrode voltammogram at v_f=0.122 mL/s. $D_{+2}=2.2\times10^{-5}$, $D_{+}=3.0\times10^{-5}$ and $D_0=4.0\times10^{-5}$ cm²/s were used for simulation.

voltammetry as well as normal pulse polarography for the solutions electrolyzed. Two unequal plateau currents seen in Figure 4 were, however, observed at the rotating disk voltammograms and pulse polarogrames when the experiments were performed in the present of sufficient amount of supporting electrolytes with the solution containing methyl viologen dication only.[18]

Figure 6 shows the simulated channel electrode voltammograms for the geometry in the experimental section by using the method described in the above for v_f=0.122 mL/s. $K_{comp}(=k_f/\kappa_b)$ of 6×10^6, which was determined from the difference of the redox potentials ΔE=0.4/V, was used to simulate the voltammograms. The voltammogram was insensitive to D_o as expected. The limiting current at the second plateau strongly depended on the comproportionation kinetics and increases as κ_f becomes larger because slowly diffusing A is replaced by two molecules of rapidly diffusing B

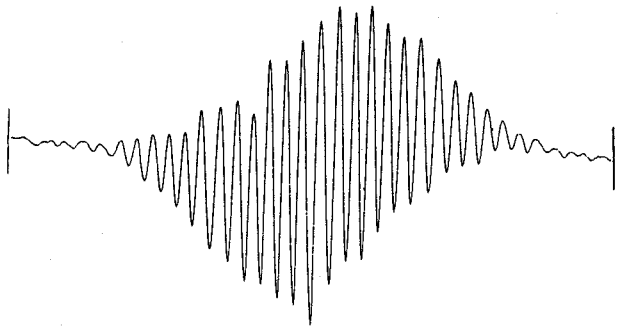

Figure 7. ESR spectrum obtained by electroreduction (at −0.6 V versus AgQRF). The conditions are the same as Figure 3.

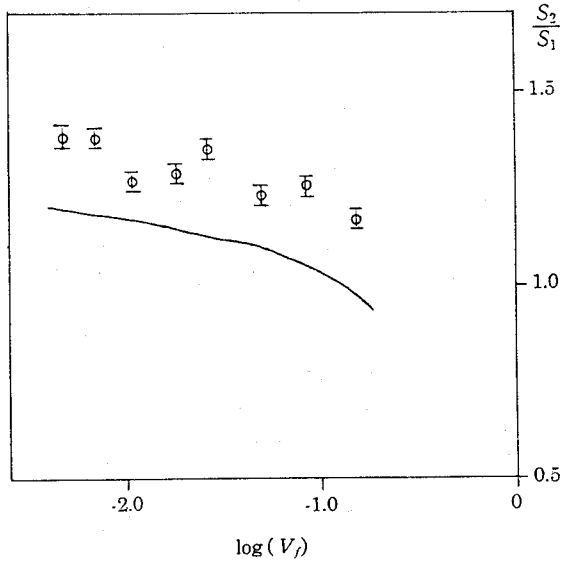

Figure 8. Experimental (Φ) and simulated (−) plots of the ratio of ESR signals versus log (flow rate). $D_{+2}=2.2\times10^{-5}$, $D_{+}=3.0\times10^{-5}$ and $D_0=4.0\times10^{-5}$ cm²/s and $\kappa_f=6\times10^8$ mol/cm³/s were used for simulation.

as the rate of comproportionation increases. Upper value of κ_f was limited to 10^9 cm³/mol·s in the present study because of the computational capability. The experimental limiting current for the second step is still much larger than the simulated one. Thus we conclude $\kappa_f>10^6$ $M^{-1}S^{-1}$, which agrees with the literature values of 3×10^9 $M^{-1}S^{-1}$[5,6] and $>10^7$ $M^{-1}S^{-1}$.[7]

ESR studies were next conducted using the flow cell described above with the electrode at potentials of the first plateau current (I) and positioned at the center of the ESR cavity. The ESR spectrum shown in Figure 7 is similar to those reported previously[19,20] except coalence of the fine splitting into an envelope spectrum because of increased dipolar broadening and spin exchange at the concentrations used in our flow system. The dependence of the steady-state ESR signal (S_1) on the current (log(S_1/I)) and the flow rate (log v_f) was linear with a slope of −2/3, which has been theoretically derived and experimentally verified for stable electrogenerated radicals in the convective systems of channel electrode[12,21] as well as tube electrode.[16] The potential was then

stepped to those of the second plateau current and the changed ESR signal (S_2) was recorded again as a function of solution flow rate. Figure 8 shows the experimental and simulated plots of S_2/S_1 versus log (v_f). The experimental fact that S_2 is larger than S_1 at a given flow rate manifests that concentration of the viologen radical generated *via* comproportionation (3) at the potential of the second plateau is greater than the one generated directly at the electrode surface at the potential of the first plateau and that the monocation radical so produced is stable inside the channel flow cell during the time of measurements. It should be noted that S_2 dose not reach twice S_1. This is because neutral viologen is electrochemically generated at the potential of the second plateau and diffuses into the bulk solution containing viologen monocation radicals. Simulated (S_2/S_1) versus log (v_f) increased as larger comproportionation rate constant was used. With $\kappa_f = 10^9$ $cm^3/mol \cdot s$, the largest comproportionation rate constant employed in the simulation, the simulated (S_2/S_1) was lower than the experimental values in the electrolyte flow range $1.3\times10^{-1} \geq v_f \geq 2.7\times10^{-3}$ cm^3/s. Accordingly, here again we reach the same result of $k_f > 10^6$ $M^{-1}S^{-1}$, as was obtained with channel electrode voltammetry in the above.

In conclusions, we have developed BIFD method for channel electrode voltammetry and in situ electrochemical ESR on reversible comproportionation kinetics at channel flow cells. Two separated unequal plateau currents of the first and second redox processes of methyl viologen dication were observed from the channel electrode voltammograms. Digital simulation analysis of channel electrode voltammogram and in situ electrochemical ESR data shows that the comproportionation rate constant is greater than 10^6 $M^{-1}S^{-1}$ and is effectively diffusion-controlled on the channel electrode timescale.

Acknowledgment. CWL was a KOSEF-RS Visiting Fellow and thanks Korea Uneversity and the Ministry of Education, Korea, for financial support. JCE and RAWD thank the EPSRC and NERC respectively for Research Studentships, and St. Hugh's College and St. Edmund Hall respectively for Senior Scholarships.

References

1. Lee, C-W.; Jang, J.-M. *Bull. Korean Chem. Soc.* **1994**, *15*, 563.
2. Lee, C-W.; Oh, M.-K.; Jang, J.-M. *Langmuir* **1993**, *9*, 1934.
3. Compton, R. G.; Waller, A. M.; Monk, P. M. S.; Rosseinsky, D. R. J. *Electroanal. Chem. Interfac. Electrochem.* **1989**, *267*, 309.
4. Compton, R. G.; Coles, B. A.; Spackman, R. A. *J. Phys. Chem.* **1991**, *95*, 4742.
5. Winograd, N.; Kuwana, T. *J. Am. Chem. Soc.* **1970**, *92*, 225.
6. Rosseinsky, D. R.; Monk, P. M. S. *J. Chem. Soc. Faraday. Trans.* **1990**, *86*, 3597.
7. Norton, J. D.; White, H. S. *J. Electroanal. Chem. Interfac. Electrochem.* **1992**, *325*, 341.
8. Laasonen, P. *Acta Math.* **1949**, *81*, 309.
9. Anderson, J. L.; Moldoveanu, S. *J. Electroanal. Chem. Interfac. Electrochem.* **1984**, *179*, 107.
10. Lapidus, L.; Pinder, G. F. *Numerical Solution of Partial Differential Equations in Science and Engineering*; Wiley: New York, 1982; Chap. 4.
11. Levich, V. G. *Physicochemical Hydrodynamics*; Prentice Hall, Englewood Cliffs, 1962; Chap. 2.
12. Coles, B. A.; Compton, R. G. *J. Electroanal. Chem. Interfac. Electrochem.* **1983**, *144*, 87.
13. Webster, R.; Dryfe, R. A. W.; Eklund, J. C.; Lee, C.-W.; Compton, R. G. *J. Electroanal. Chem. Interfac. Electrochem.* in press.
14. Compton, R. G.; Waller, A. M. *J. Electroanal. Chem. Interfac. Electrochem.* **1985**, *195*, 289.
15. Compton, R. G.; Coles, B. A.; Day, M. *J. Electroanal. Chem. Interfac. Electrochem.* **1986**, *200*, 205.
16. Albery, W. J.; Coles, B. A.; Couper, A. M. *J. Electroanal. Chem. Interfac. Electrochem.* **1975**, *65*, 901.
17. Rongfeng, Z.; Evans, D. H. *J. Electroanal. Chem. Interfac. Electrochem.* **1995**, *385*, 201.
18. Oh, M.-K.; Lee, C.-W. unpublished results.
19. Johnson, Jr. C. S.; Gutowsky, H. S. *J. Chem. Phys.* **1963**, *39*, 58.
20. Rieger, A. L.; Rieger, P. H. *J. Phys. Chem.* **1984**, *88*, 5845.
21. Compton, R. G.; Waller, A. M. In *Spectroelectrochemistry*; Gale, R. J., Ed.; Plenum Press: New York, 1988; p 349.